STAGNATION POINT HEAT TRANSFER WITH GAS INJECTION COOLING

B. Vancrayenest[*,†], **M. D. Tran**[*], **and D. G. Fletcher**[*]

[*]von Karman Institute for Fluids Dynamics, Chaussée de Waterloo 72, 1640 Rhode-Saint-Genèse, Belgium,
Email: vancraye@vki.ac.be

[†]Centre National d'Études Spatiales, 18 avenue Edouard Belin, 31401 Toulouse, France

ABSTRACT

The present paper deals with an experimental study of the stagnation-point heat transfer to a cooled copper surface with gas injection under subsonic conditions. Test were made with a probe that combined a steady-state water-cooled calorimeter that allows the capability to study convective blockage and to perform heat transfer measurements in presence of gas injection in the stagnation region. The copper probe was pierced by 52 holes, representing 2.4% of the total probe surface. The 1.2 MW high enthalpy plasma wind tunnel was operated at anode powers between 130 and 230 kW and a static pressures from 35 hPa up to 200 hPa. Air, carbon dioxide and argon were injected in the mass flow range 0-0.4 g/s in the boundary layer developed around the 50 mm diameter probe. The measured stagnation-point heat transfer rates are reported and discussed.

1. INTRODUCTION

One type of thermal protection system, which is used by many capsules and probes employs ablative composite material. At high temperatures the organic resin decomposes and vaporizes, absorbing some of the thermal energy; this process is known as pyrolysis. The pyrolysis gas is then injected into the flow creating a thin layer of cooled gas over the vehicle which blocks additional thermal load. The effect of blowing mass through porous walls, holes or slits has been studied in the literature but shows a large scattering of data. Related to the ablation re-entry flow regime, the convective blockage is the topic of this study. The release of pyrolysis gas will be simulated by injecting gas into the flow through multiple ports; this is known as transpiration cooling. The goal of this project is to investigate the reduction in heat flux caused by transpiration cooling for a probe in a subsonic plasma flow. Attempts will be made to correlate the change in heat flux to the mass flow rate and composition of the gas injected.

Extensive plasma tests were performed for different transpiration and plasma conditions. Different gases such as air, argon, and carbon dioxide were injected through the surface of the probe into the air plasma flow. The probes were also instrumented to measure temperatures, pressures, and heat flux within the probe. A significant part of this effort was focused on the development and verification of the gas injection system.

2. FACILITIES AND TESTING

The Plasmatron is a high enthalpy facility in which a jet of plasma is generated in a test chamber kept at sub-atmospheric pressure (typically between 7 and 200 mbar). The plasma is generated by heating a gas (in the present study, only air plasma was considered) to temperatures up to about 10.000 K, using electrical current loops induced inside a 160 mm diameter plasma torch. The inductively-coupled plasma wind tunnel uses a high frequency, high power, high voltage (400 kHz, 1.2 MW, 2 kV) solid state (MOS technology) generator.

The accurate quantitative measurement of heat transfer rates in high enthalpy plasma facilities has always been a challenging task. Coupling gas injection systems with this type of measurement is even more difficult because of the need for the same space. The multi-point gas injection probe (Fig. 1) was based off the 14 mm diameter water-cooled calorimeter, which has been used successfully in the past at VKI to measure heat fluxes. In addition to measuring heat flux, this probe must inject gas uniformly into the plasma stream at the stagnation point for known conditions. The settling chamber for the gas had to be immediately after the front face; therefore, the water chamber could only be placed after the settling chamber. Thus, heat would is transferred by conduction through the copper side walls to the calorimeter. Since this heat conduction path from the front face to the water calorimeter has to be short and to allow for sufficient circulation in the water calorimeter, the volume of the gas settling chamber was significantly reduced (this raised concern over

whether the injected gas would still be uniform across the front face. In order to assess the validity of this assumption, velocity profiles using hot wire velocimetry were performed latter and showed reasonable uniformity within 1 mm of the surface).

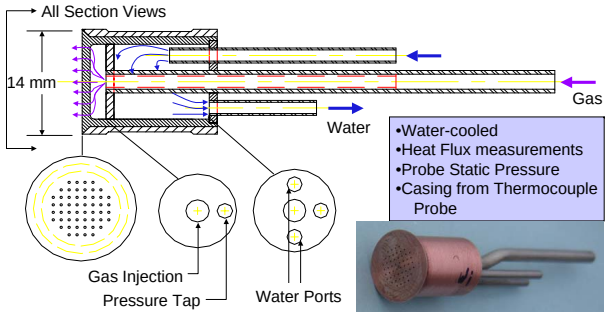

Figure 1. Steady-state water-cooled calorimeter with gas injection

In [4], different amounts of holes for the gas injection on the front face were tested: 21, 37, 57, and 77. The probe with 21 holes showed significantly less heat transfer efficiency compared to the others. There was little difference, however, between the 37 and 77 holes. Therefore, The 52 holes configuration was chosen, with a hole diameter of 0.3 mm (for a 2 mm gas injection pipe diameter) and a 1 mm distance between the holes, giving approximately a 2 hole diameter spacing between the holes.

A teflon piece is used to separate the probe from the holder. It limits heat flux loss due to conduction through the sidewalls, which are then considered negligible. For the water calorimeter, conduction losses due to the proximity of the water inlet and outlet pipes must also be considered. The radiated heat flux of the cold-wall probe is also considered small, since the probe wall is kept at a low surface temperature. This effect was measured using a Gardon gage for air and CO_2 plasma at various static pressures. For the most extreme case, CO_2 at 70 mbar, maximum radiative loss was 5.4% of the total heat flux and represented, on average 4.6%.

The probe was inserted into the ESA sample holder, 50 mm diameter cylindrical blunt body. The gas was injected through a port in the back of the probe. The mass flow rate of the transpiration gas was measured using a G0-100 rotameter with a range of 0 to 1 g/s. The pressure transducer was located inside the arm of the model, so the gage pressure would be measured relative to the Plasmatron test chamber pressure. The mass flow of the cooling water is measured using a L16-630 rotameter. The pressure transducer for the pressure tap in the probe was an SM5415 with a 15 psi (1030 mbar) range. The rotameter for the transpiration gas was also switched after the initial tests. The G0-100 was used for the initial tests from 0.1 to 0.4 g/s. For measurements at a lower mass flow, the rotameter was switched to the L16-630 which has a range from 0 to 0.4 g/s.

3. EXPERIMENTAL RESULTS

Fig. 2 shows the heat flux measurements for air as the transpiration gas. The initial tests with the G0-100 rotameter were performed for the flow rates between 0.1 and 0.4 g/s. The results from these tests were as expected, as the transpiration mass flow rate was decreased the heat fluxed increased. Injected mass flow was found to be too high to study the region where the rise of heat flux is exponential as in [4], so the smaller rotameter was used to measure lower mass flow rates between 0 to 0.1 g/s. In Fig. 2, one can note differences in the two heat flux measurements at 0.1 g/s which can mostly be explained by this switch in rotameters. This difference will be discussed later in the uncertainties of the rotameter calibration.

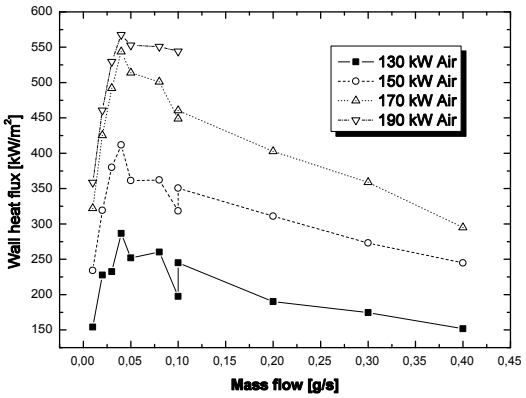

Figure 2. Heat flux vs. transpirational $\dot{m}_{air}$

The heat flux was found to unexpectedly decrease for low mass flow rates. The monotonic behavior observed in [4] was not reproduced. For all the power settings, the heat flux rises to a maximum heat flux at 0.04 g/s. For flow rates below 0.4 g/s, the heat flux decreases with decreasing transpiration flow rates, but then rises again somewhere between 0 and 0.01 g/s. Fig. 3 and 4 are the heat flux plots for carbon dioxide and argon (zero mass flow values in Fig.4 were obtained turning off the gas injection). They exhibit the same trend as air. The heat flux always reaches a maximum at 0.04 g/s.

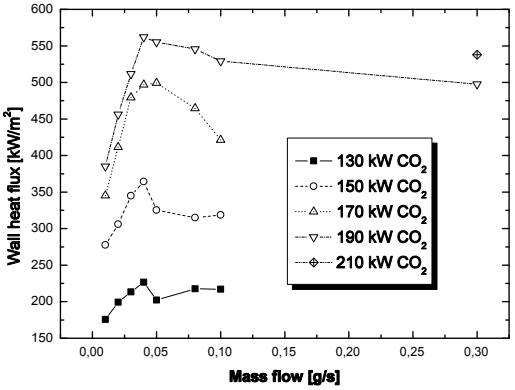

Figure 3. Heat flux vs. transpirational $\dot{m}_{CO_2}$

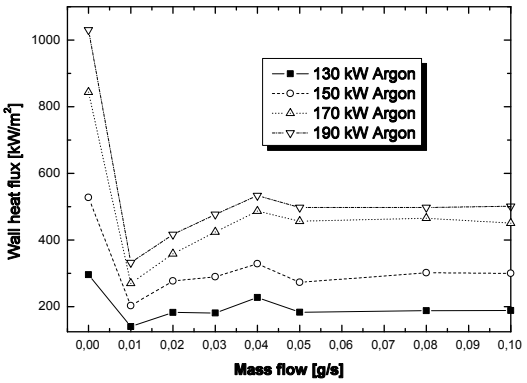

Figure 4. Heat flux vs. transpirational $\dot{m}_{argon}$

4. DISCUSSION OF RESULTS

Sensitivity studies for the injected gas pressure were performed in the transpiration gas rotameter and also for the static pressure in the test chamber. For the last test case with nitrogen, a thermocouple was added to the gas injection pipe of the probe to determine whether the gas was getting preheated before reaching the settling chamber. The temperature measurements varied between 24 to 34 $^\circ$C, so its effect was determined to be negligible.

Pressure measurements inside the settling chamber of the probe were also made. These measurements were taken to determine the conditions of the gas before being injected. Unfortunately, the temperature of the gas could not be measured so that the gas in the settling chamber could not be completely characterized.

The pressure measurements could also be used to determine whether the velocity in the injection holes reached sonic flow using the following equation:

$$\frac{p_0}{p} = \left(1 + \frac{\gamma - 1}{2} M^2\right)^{\gamma(\gamma-1)} \tag{1}$$

where γ equals 1.4 for air, 1.29 for carbon dioxide, 1.4 for nitrogen, and 1.67 for argon. To check for the onset of sonic conditions, Mach number M, is set to 1. Even though the holes are choked, mass flow through the holes can still be increased because according to mass flow rate at a choked throat can be found by:

$$\dot{m}^* = \left(\frac{2}{\gamma + 1}\right)^{(\gamma+1)/[2(\gamma-1)]} \sqrt{\gamma/R} \frac{A^* P_0}{\sqrt{T_0}} \tag{2}$$

This equation shows that for a choked flow the mass flow rate is directly proportional to the throat area and the stagnation pressure and inversely proportional to the square root of the stagnation temperature. Therefore, if the stagnation pressure is increased the mass flow rate is increased. Choking seemed to be a possible cause for the unexpected heat flux measurements so the pressure ratios were increased by raising the test chamber static pressure to 200 mbar. Still the heat flux plot had the same trend. Therefore, possible sonic flow in the holes appears to not affect the trend in heat flux. Fig. 5 compares test chamber result for the static pressures of 200 mbar with nitrogen as the transpiration gas and 35 mbar for the other transpiration gases. The case for nitrogen at 35 mbar is not shown since a leak is suspected for this run. It should be similar to the other gases though, especially air which is 79% nitrogen.

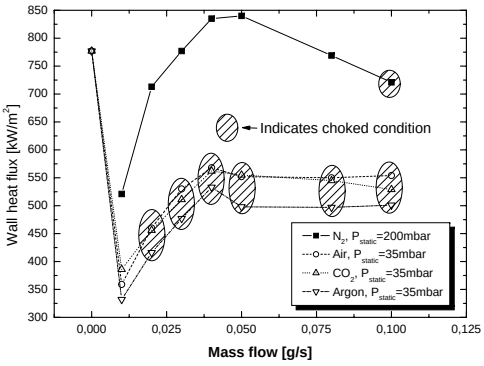

Figure 5. Heat flux with and without chocking

The plots of the heat flux show three distinct regions. Although data points were not measured in the first region due to the limitations of the rotameter, heat flux was measured for mass flow rates of 0

and 0.01 g/s. From these two points, we can conclude that in general the heat flux decreases with increased transpiration mass flow within this range. For mass flows between 0.01 to 0.04 g/s, the heat flux rises with increased transpiration mass flow. For mass flows above 0.04 g/s, the heat flux becomes more constant, only slightly decreasing with increased transpiration mass flow. A reasonable explanation was established after a survey of film cooling [1] and a review of the videos from the tests.

Film cooling, typically for turbine blades, is similar to transpiration cooling in that gas is injected into the flow through many holes or slots. The difference is that film cooling is specifically for crossflows and generally intended to protect regions downstream of the flow. Still certain analogies can be made for transpiration and film cooling, and much more literature is available for film cooling.

For film cooling, there are two flow regimes: low and high injection rates. Injection rates are characterized by a blowing ratio M, defined as:

$$M = \frac{\rho_{gas} U_{gas}}{\rho_\infty U_\infty} \tag{3}$$

where, the $(\cdot)_{gas}$ subscript is for injected gas properties and the $(\cdot)_\infty$ subscript for freestream conditions. At low injection rates, the momentum of the impinging jet causes the injected gas to immediately bend along the surface of the probe. This creates a thin film over the surface which is very effective at cooling the surface. At high injection rates the jet penetrates into the mainstream and eventually separates from the wall. This is not as effective at cooling the surface.

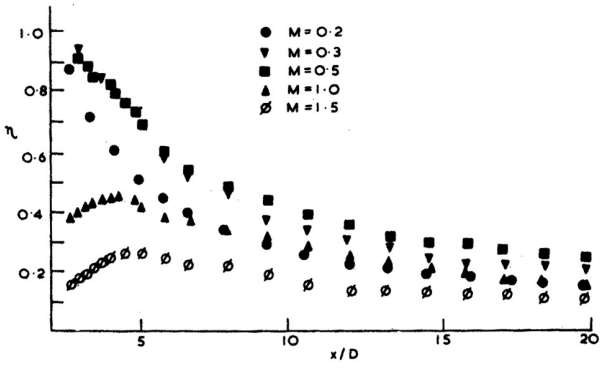

Figure 6. Effect of blowing ratio for film cooling

For the case of film cooling, there exists an optimum blowing ratio, where the injected mass flux is high yet the jet remains attached to the wall. For example in Fig. 6 from [1], the optimum blowing ratio for this particular case was around 0.5. In this graph, η is defined as the wall film cooling effectiveness and x/D is a streamwise coordinate. We are not concerned with x/D for our study, but concentrating on one coordinate, you can see that effectiveness at first increases for higher blowing ratios then decreases after about 0.5.

A similar situation could be argued for the current results. The dynamic pressure of the plasma jet at the location of the probe has been measured using a pitot probe and values are low (62.44 Pa for the 130 kW and 75.47 Pa for 150 kW). The velocities measured for the injected gas, on the other hand, were fairly large even in atmospheric conditions. Also, since the plasma jet is in a low pressure and high temperature condition the density of the gas is much lower. Ultimately, this leads to a high blowing ratio which means the transpiration flow could well be penetrating into the plasma jet. The carbon dioxide injection was shown to be an excellent tool for visualizing the transpiration flow and the carbon dioxide run videos support this hypothesis as seen in Fig. 7.

By dividing the mass flow rate of the transpiration gas by the area of the injected holes, the numerator of the blowing ratio can be determined. The denominator of the blowing ratio can be found using the dynamic pressure and plasma mass flow rate information. The blowing ratio M, for transpiration mass flow rate of 0.01 g/s and 0.10 g/s is approximately 3 and 30, respectively. Blowing ratios for the Mars Pathfinder were estimated according to results from a numerical study [2]. Based on a given trajectory and heat shield made of silicone elastomeric charring ablator, known as SLA-561V, the maximum blowing ratio was approximately 0.01.

Although heat flux measurements were not taken at the low flow rates of the first region, there must be a steep decrease in heat flux with increasing mass flow, because the heat flux for zero mass flow is significantly larger than for 0.01 g/s. In this region, the transpiration gas encounters the impinging plasma jet causing a thin film of cool, transpiration gas to envelope the surface. This convective blockage shields the probe from the heat load, decreasing the heat flux the probe experiences. As the transpiration mass flow increases in this regime, the film becomes thicker and there is more mass to transport the heat load, so the heat flux continues to decrease.

For mass flows in the second regime, the jets from the transpiration probe are penetrating into the plasma jet. This is shown in Fig. 7, where the jets from the transpiration probe are creating a cone shape. This is a less effective heat shield because the transpiration gas is being used to cool a larger volume rather than a thin layer over the most critical region where heat transfer is the highest. The transpiration gas is not as effective at cooling this larger volume, and it is the hotter gases in this recirculation region that are now in contact with the surface of the probe. As the injection rate is increased in this regime, the heat flux increases because the transpiration jets are penetrating further into the plasma jet increasing the volumes and becoming less effective.

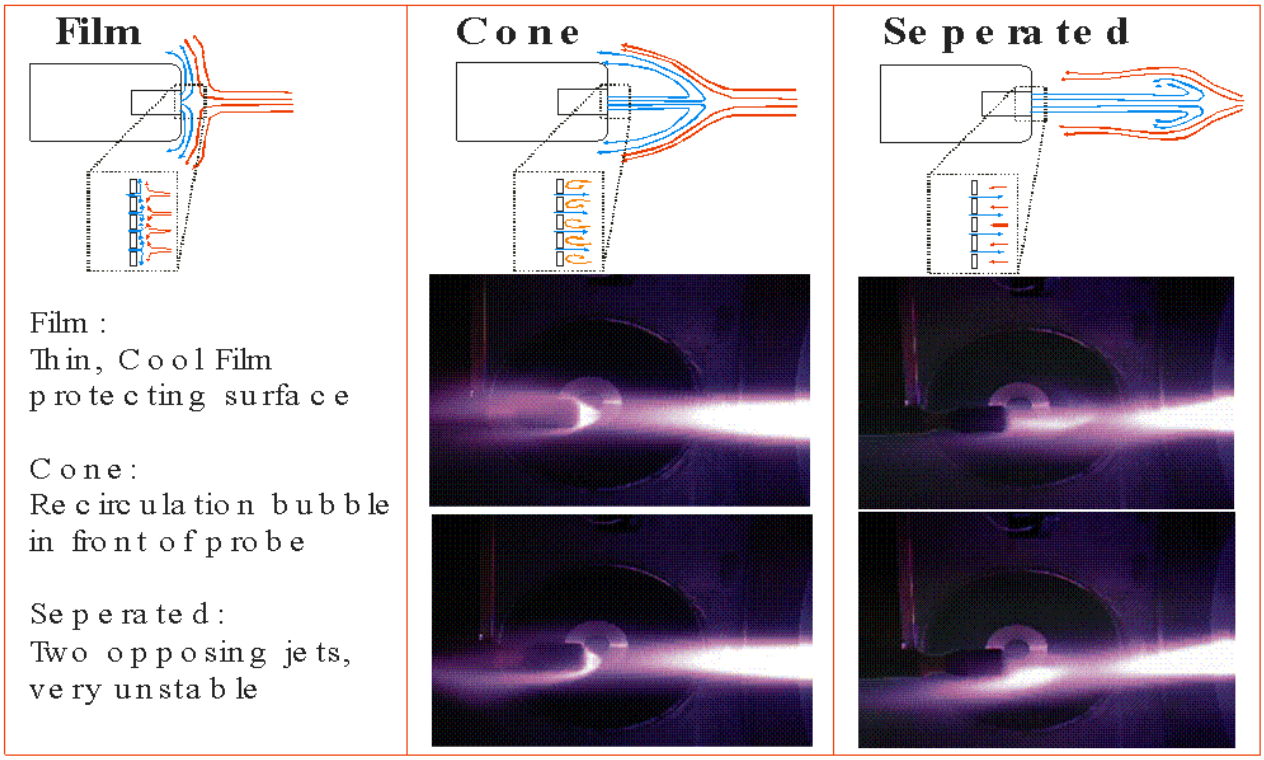

Figure 7. Three flow regimes

In the third regime, the jets of transpiration gas have penetrated so far into the plasma jet that the cone has become detached. A region covering the probe surface is no longer defined. Instead, the transpiration gas is a jet in front of the probe. Heat from the plasma flow can come in direct contact with the surface due to instabilities in the opposing jets. Increases in injection rates decrease heat flux only slightly since the additional mass is less effective so far away from the probe surface.

The results from [4] showed an exponential decrease in heat flux with increasing mass flow rates. This would correspond to the results expected for the first regime. Unfortunately, we were not able to achieve blowing ratios that low.

5. HEAT FLUX MEASUREMENT UNCERTAINTIES

To calculate the heat flux the probe experiences the following energy balance, as discussed previously, is applied:

$$q_w = \frac{\dot{m} \cdot Cp \cdot (T_{out} - T_{in})}{A} \tag{4}$$

Therefore, the uncertainties in the heat flux measurements arise for a combination of the uncertainties in the measurement chain with:

- $\dot{m}$ is the mass flow rate of the water through the calorimeter, measured with a ROTA L16/630-6404. Uncertainty of mass flow rate will typically be $\delta(\dot{m}) = 1/50 = \pm 0.02$ g.
- Cp is the specific heat of water. For the range of temperatures the water experiences, the change in Cp was estimated to be $\delta(Cp) = 0.01$ J/kg-K.
- T_{out} and T_{in}, are the temperatures at the outlet and inlet of the calorimeter. The temperatures are measured using thermocouples.
- A, is the area of the sensing element. The diameter of the face is 14 mm and uncertainty in the diameter is estimated to be ± 0.1 mm. $\delta(T_{read,in}) = \pm 0.3$ $^\circ$C, uncertainty in temperature going into the calorimeter. $\delta(T_{read,out}) = \pm 0.7$ $^\circ$C, uncertainty in temperature leaving the calorimeter.

The most probable error in a measurement can be calculated using the following equation:

$$\left(\frac{\delta q}{q}\right)^2 = \left(\frac{\delta \dot{m}}{\dot{m}}\right)^2 + \left(\frac{\delta Cp}{Cp}\right)^2 + \left(\frac{\delta A}{A}\right)^2 + \left(\frac{\delta T_{in}}{\Delta T}\right)^2 + \left(\frac{\delta T_{out}}{\Delta T}\right)^2 \tag{5}$$

where ΔT is the temperature difference between $T_{out} - T_{in}$.

Table 1. Breakdown of heat flux uncertainties.

Breakdown of Uncertainties Percentage of Uncertainty/Total Heat flux						
Run	$\dot{m}_w$	Cp_w	A	T_{out}	T_{in}	total
Air	1,8	0,2	1,4	6,9	2,9	13,3
CO2	1,5	0,2	1,4	7,5	3,2	13,8
Argon	2	0,2	1,4	6,3	2,7	12,6
Combined	1,7	0,2	1,4	6,9	2,9	13,2

Table 1 shows a breakdown of the uncertainties. For each test condition, the uncertainties were calculated then divided by the total heat flux measured to obtain a percentage. These percentages were then averaged for the different gases tested. The last row shows the average of the three runs. The temperature measurements are the largest source of error, because the fluctuations in the temperature make it difficult to determine the steady state value. The last column shows the total uncertainty for the measured heat flux.

6. IMPROVEMENTS AND FURTHER STUDIES

In order to be able to perform measurements in the first transpiration film cooling regime which is more representative of ablating re-entry flight conditions, the easiest way to proceed is to decrease the transpiration mass flow. Adaptations to the existing setup are currently in progress. Another way to measure this first regime accurately without having to go to lower transpiration mass flow rates would be to decrease the blowing ratio but working conditions affecting this ratio are more uncertain.

As mentioned previously in the probe design section, the heat flux measured is only relative to the front face, because there is a cool layer of gas in between the majority of the area between the front face and the calorimeter. The heat is primarily transferred to the calorimeter through the cooper walls. Heat pipes could be implemented but one can imagine that the best option for the next generation of combined transpiration/heat flux probe is to eliminate the settling chamber behind the front face and make it coaxial with the heat flux sensor. The front face and the water/slug calorimeter could be made of the same block. The front face could be made thicker so that ducts can be machined into it to feed the injection holes. In this way, the calorimeter would be covered by a thicker that will create the settling chamber for the injected gas.

7. CONCLUSIONS

The goal of this study was to gain experience in transpiration cooling in a subsonic plasma stream. This was achieved by a multistage design and test approach. The probes were able to inject gas uniformly into the plasma flow. This was verified by measuring the velocity profiles of the injected gas. The probes successfully measured conditions of the gas (temperature, pressure, and heat flux) before being injected into the flow. Relationships were then developed and verified for various plasma conditions, transpiration gases and mass flow rates in the Plasmatron facility.

Some of these results were unexpected. However they do appear to be consistent with other research on film cooling. Through this investigation, it was determined that the tests were performed at higher blowing ratios than expected, and the transpiration gas was actually penetrating the plasma jet. Recommendations were made for improvements and verification of the three flow regimes assumption.

New probe designs for the Plasmatron facility are never straightforward. By taking a multistage approach, though, we have successfully gained experience in transpiration cooling in a subsonic plasma flow. Eventually, this probe and knowledge will be applied to ablation research for a better understanding of pyrolysis gas injection.

8. ACKNOWLEDGEMENTS

This work was supported by funding from the Belgian Federal Office for Scientific, Technical and Cultural Affairs through a grant from ESA, administered by CNES (Dr J.M. Charbonnier technical monitor). The support of M. Tran by USAF fellowship is gratefully acknowledged.

REFERENCES

G. G. Bergeles, A. D. Gosman, and B. E. Launder. Near-field character of a jet discharge through a wall at 30 degrees to a maintream. *AIAA journal*, 15(4):499–504, 1977.

Y. K. Chen, W. D. Henline, and M. E. Tauber. Mars Pathfinder trajectory based heating and ablation calculations. *Journal of Spacecraft and Rockets*, 32(2):225–230, March-April 1995.

W. C. Davy, G. P. Menees, J. H. Lundell, and R. R. Dickey. *Hydrogen-helium ablation of carbonaceous materials: numerical simulation and experiment*, volume 64 of *Progress in Astronautics and Aeronautics*. Raymond Viskanta, 1978.

M. I. Yakushin, I. S. Pershin, and A. F. Kolesnikov. An experimental study of stagnation point heat transfer from high-enthalpy reacting gas flow to surface with catalysis and gas injection. In *Proceedings of the fourth European Symposium on Aerothermodynamics for Space Vehicles*, pages 473–479, Capua, Italy, 15 - 18 October 2001.